Reprinted from THE JOURNAL OF CHEMICAL PHYSICS, Vol. 40, No. 4, 939–950, 15 February 1964
Printed in U. S. A.

Fifth and Sixth Virial Coefficients for Hard Spheres and Hard Disks*

FRANCIS H. REE AND WILLIAM G. HOOVER
Lawrence Radiation Laboratory, University of California, Livermore, California

(Received 12 August 1963)

New expressions for the fourth, fifth, and sixth virial coefficients are obtained as sums of modified star integrals. The modified stars contain both Mayer f functions and $\tilde{f}$ functions ($\tilde{f}\equiv f+1$). It is shown that the number of topologically distinguishable graphs occurring in the new expressions is about half the number required in previous expressions. This reduction in the number of integrals makes numerical calculation of virial coefficients simpler and more nearly accurate. For particles interacting with a hard-core potential, values of the modified star integrals are shown to depend strongly on dimension; for example, several modified star integrals are identically zero for hard disks (two dimensions), but give nonzero values for hard spheres (three dimensions). Of all the modified star integrals contributing to the fourth, fifth, and sixth virial coefficients, the complete star integrals are shown to be the largest. Mayer's expressions for these coefficients made the complete star integrals the smallest contributing integrals.

The fifth (B_5) and sixth (B_6) virial coefficients of hard-sphere and hard-disk systems are obtained by Monte Carlo integration of the modified star integrals. The resulting values are

$$\text{spheres: } B_5/b^4=0.1103\pm0.0003;\quad B_6/b^5=0.0386\pm0.0004$$

$$\text{disks: } B_5/b^4=0.3338\pm0.0005;\quad B_6/b^5=0.1992\pm0.0008$$

where b is the second virial coefficient.

Estimated values of B_7 obtained from a Padé approximation to $PV^2/(N^2kT)-V/N$ are $B_7/b^6=0.0127$ for hard spheres and 0.115 for hard disks. For hard spheres virial series calculations including terms through the sixth virial coefficient give values of $PV/(NkT)$ which agree closely, for densities less than half of closest-packing, with the molecular dynamics data of Alder and Wainwright. Furthermore the approximate Padé expression agrees within 2% with the molecular dynamics data for all densities on the fluid side of the solid–fluid transition. This agreement indicates convergence of the virial series along the entire fluid branch of the hard-sphere equation of state.

I. INTRODUCTION

THE virial expansion of the pressure P of an imperfect gas is a power series expansion in the number density[1] $\rho(\equiv N/V)$,

$$PV/(NkT)=1+B_2\rho+B_3\rho^2+B_4\rho^3+\cdots, \tag{1}$$

where N is the number of particles in the volume V at a temperature T and k is Boltzmann's constant.

The nth virial coefficient B_n for a gas with the pairwise additive interaction potential ϕ_{ij} between Particles i and j can be expressed in terms of Mayer f functions[2]:

$$B_n=\frac{1-n}{n!}\lim_{V\to\infty}V^{-1}\int\cdots\int d\mathbf{r}_1\cdots d\mathbf{r}_nV_n, \tag{2}$$

$$V_n\equiv\sum_{\{S_n\}}\prod_{i>j}^{n}f_{ij}, \tag{3}$$

$$f_{ij}\equiv\exp(-\phi_{ij}/kT)-1; \tag{4}$$

where the sum in (3) includes all labeled stars with n points.

Because the number of terms in V_n, as well as the difficulty in evaluating them, grows rapidly with n, only the first few virial coefficients have been evaluated for "realistic" potentials. For the hard-sphere gas, the following exact results are known[3,4]:

spheres:

$$B_2\equiv b=(2\pi/3)\sigma^3,\qquad B_3/b^2=\tfrac{5}{8},\qquad B_4/b^3=0.28695, \tag{5}$$

where σ is the sphere diameter. An approximate value of $B_5/b^4=0.115\pm0.005$ was obtained by the Rosenbluths,[5] who used Monte Carlo integration to evaluate the 10 types of star integrals occurring in B_5. For a two-dimensional gas composed of hard disks, the first three coefficients are known exactly[6]:

disks:

$$B_2\equiv b=(\pi/2)\sigma^2,\quad\text{and}\quad B_3/b^2=\tfrac{4}{3}-\sqrt{3}/\pi=0.78200, \tag{6}$$

where σ is the disk diameter. $B_4/b^3=0.5327\pm0.0005$

* This work was performed under the auspices of the U.S. Atomic Energy Commission.

[1] For an excellent discussion of this subject, refer to G. E. Uhlenbeck and G. W. Ford, in *Studies in Statistical Mechanics*, edited by J. de Boer and G. E. Uhlenbeck (North-Holland Publishing Company, Amsterdam, The Netherlands, 1962), Vol. 1, Part B. We shall follow the graph theoretical terminologies used by these authors.

[2] J. E. Mayer and M. G. Mayer, *Statistical Mechanics* (John Wiley & Sons, Inc., New York, 1940).

[3] L. Boltzmann, Verslag Gewone Vergader. Afdel. Natuurk. Koninkl. Ned. Akad. Wetenschap. **7**, 484 (1899); H. Happel, Ann. Physik **21**, 342 (1906).

[4] B. R. A. Nijboer and L. Van Hove, Phys. Rev. **85**, 777 (1952).

[5] M. N. Rosenbluth and A. W. Rosenbluth, J. Chem. Phys. **33**, 1439 (1960).

[6] See M. Metropolis, A. W. Rosenbluth, M. N. Rosenbluth, A. H. Teller, and E. Teller, J. Chem. Phys. **21**, 1087 (1953). B_3 is calculated by L. Tonks, Phys. Rev. **50**, 955 (1936). We have checked B_4 for disks, using 10^7 Monte Carlo trial configurations, and find $B_4/b^3=0.5324\pm0.0003$.

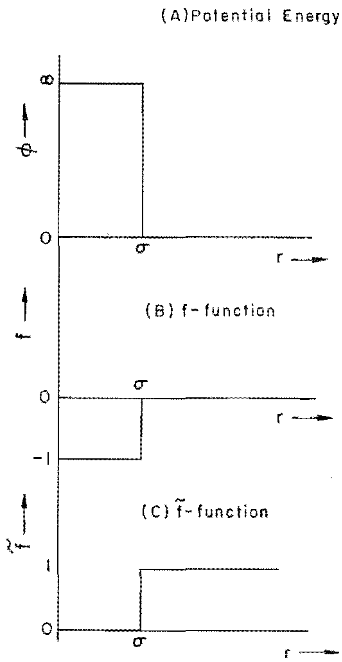

FIG. 1. (A) The hard-core potential ϕ; (B) The corresponding f function; (C) $\tilde{f}$ function.

and $B_5/b^4=0.312\pm0.016$ were obtained for disks by Metropolis *et al.*[6] using Monte Carlo integration.

As was observed by the above authors and also by Hoover and De Rocco[7] in calculating $B_{n\leq 7}$ for the parallel hard-square and hard-cube models, the contribution of star integrals with positive values to $B_{n\geq 4}$ is approximately equal to the contribution of star integrals with negative values. The final value for B_n is about the same order of magnitude as the contribution of a complete star integral alone; the complete star integral has the smallest absolute value of all the star integrals involved in calculating B_n. We present, in the following section, an alternative way of evaluating the virial coefficients. This new approach is particularly useful in the numerical calculation of virial coefficients beyond the third. In Secs. 3 and 4, this method is used to evaluate B_5 and B_6 for hard spheres and hard disks. It is found that the main contribution to B_5 and B_6 comes from the complete star integral, while other graphs, some positive and some negative, give smaller corrections. It is also shown that (depending on the dimensionality of the particles) some of the modified star integrals in this formalism are identically zero. In Sec. 5, we estimate B_7 for hard spheres and hard disks, and discuss the convergence of the virial series along the fluid branch of the equation of state.

2. MODIFIED STARS

We introduce the function $\tilde{f}_{ij}$ defined by the equation

$$\tilde{f}_{ij}\equiv \exp(-\phi_{ij}/kT) \tag{7}$$

and related to f_{ij} by the equation

$$1=\tilde{f}_{ij}-f_{ij}. \tag{8}$$

Whenever two points i and j in a star are not connected by f_{ij}, we use (8) to introduce $\tilde{f}_{ij}-f_{ij}$ into the star. When this procedure is carried out for all unconnected pairs of points in any particular star and the resulting expression is expanded, we find that the star can be written as a sum of modified stars composed of two kinds of lines, f_{ij} (denoted by a straight line between i and j), and $\tilde{f}_{ij}$ (denoted by a wiggly line between i and j). When this procedure is applied to all of the labeled stars occurring in a particular B_n, many of the graphs cancel out identically. Details of the expansion for the four-, five-, and six-point stars are given in Appendix I. The final expressions for V_4, V_5, and V_6 are as follows:

(9)

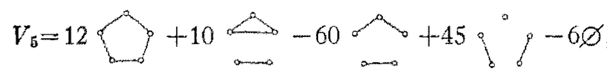

(10)

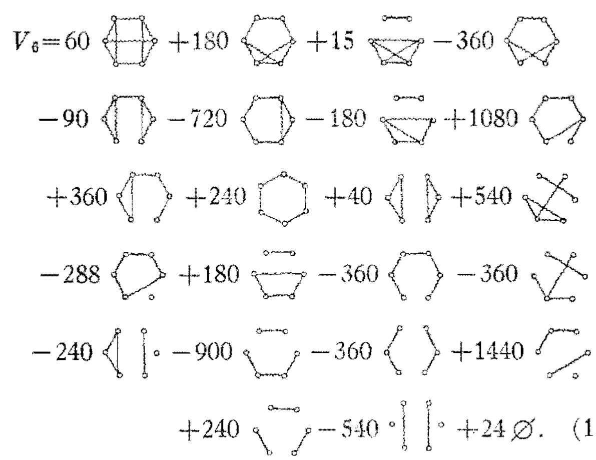

(11)

For clarity, we have omitted drawing the f functions in (9), (10), and (11). This means, for example, that

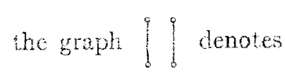

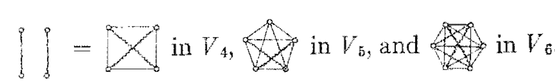

(12)

As a second example, the graph ∅ in (9), (10), and (11) denotes complete stars of four, five, and six points, respectively. For V_4, V_5, and V_6 there are, respectively, 3, 10, and 56 topologically different types of stars,

[7] W. G. Hoover and A. G. De Rocco, J. Chem. Phys. **36**, 3141 (1962).

while here we see that the corresponding modified expressions (9), (10), and (11) contain, respectively, 2, 5, and 23 topologically different types of modified stars. It is not possible at present to predict, in the general case, the type of modified stars which will occur in V_n, nor can we predict the multiplicative factors which will be associated with these modified stars. [Since this work was finished, we have obtained a new formalism, which gives all multiplicative factors corresponding to each modified star appearing in the expression of B_n. This new formalism will be reported in a later paper.] It is, however, possible to calculate the multiplicative factors for the complete star graph and the graph , in general, by using some identities obtained by Riddell and Uhlenbeck.[8] The multiplicative factors are

$$M(\varnothing)=\sum_{k=n}^{\frac{1}{2}n(n-1)}(-)^{\frac{1}{2}n(n-1)-k}S(n,k)$$

$$=-(-)^{\frac{1}{2}n(n-1)}(n-2)!, \tag{13}$$

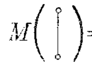

$$M(\ldots)=\sum_{k=n}^{\frac{1}{2}n(n-1)-1}(-)^{\frac{1}{2}n(n-1)-k}[\tfrac{1}{2}n(n-1)-k]S(n,k)=0, \tag{14}$$

where $S(n, k)$ denotes the number of labeled stars of n points and k lines (f functions). We also notice that the sum of the positive coefficients of modified stars contributing to V_n is always one greater than the sum of the negative coefficients of such modified stars.

3. HARD SPHERES AND HARD DISKS

For particles interacting with the hard-core potential of Fig. 1(A), the corresponding f and $\tilde{f}$ functions are shown in Figs. 1(B) and 1(C). In this section we consider the contribution of the modified stars to B_n in one-, two-, and three-dimensional systems. First, let us consider a system of N hard lines of length σ in a one-dimensional volume V. In 1934, Herzfeld and Mayer[9] obtained the equation of state for this system:

$$PV/(NkT)=(1-\sigma\rho)^{-1}. \tag{15}$$

We can easily evaluate the contribution of the complete star integrals in the new formalism to the B_n's for this system. From (2) and (13), these contributions are

$$B_n(\varnothing)=(-)^{\frac{1}{2}n(n-1)}(\varnothing)_n/n, \tag{16}$$

$$(\varnothing)_n=\lim_{V\to\infty}V^{-1}\int\cdots\int d\mathbf{r}_1\cdots d\mathbf{r}_n\prod_{i>j}^{n}f_{ij}. \tag{17}$$

[8] R. J. Riddell, Jr., and G. E. Uhlenbeck, J. Chem. Phys. **21**, 2056 (1953).

[9] K. F. Herzfeld and M. G. Mayer, J. Chem. Phys. **2**, 38 (1934).

The expression (17) can be easily evaluated[7]:

$$(\varnothing)_n=(-)^{\frac{1}{2}n(n-1)}n\sigma^{n-1}. \tag{18}$$

Therefore, we note from (16) and (18) that the B_n obtained by expanding (15) are identical to the $B_n(\varnothing)=\sigma^{n-1}$. This implies that the other modified star integrals contributing to the B_n sum to zero. In one dimension all of the four-, five-, and six-point modified star integrals contributing to B_4, B_5, and B_6 (except the complete star integrals) are zero for geometrical reasons. We conjecture that this is true for all of the higher virial coefficients as well.

We consider next a two-dimensional system of N hard disks of diameter σ. Several modified star integrals give zero contributions to the corresponding virial coefficients. We introduce a notation, $(\ )_n$, for a linear integral operator for the n particles of any graph given inside the parentheses; for example,

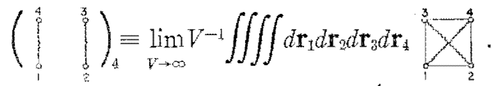

$$(\ldots)_4\equiv\lim_{V\to\infty}V^{-1}\iiiint d\mathbf{r}_1d\mathbf{r}_2d\mathbf{r}_3d\mathbf{r}_4\ \ldots\ . \tag{19}$$

The following modified star integrals represent geometrically inaccessible configurations for disks in two dimensions, and consequently vanish (see Appendix II):

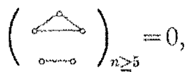

(20)

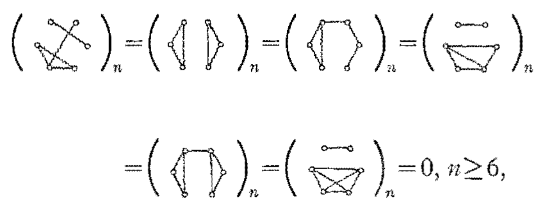

(21)

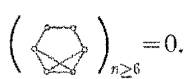

(22)

Notice that the diagrams in (21) contain at least one triangular set of $\tilde{f}$ functions $\tilde{f}_{ij}\tilde{f}_{jk}\tilde{f}_{ki}$. If, in addition to such a triangle, a modified star contains any wiggly line not linked to the triangle by fewer than two intermediate wiggly lines, the corresponding modified star integral vanishes for hard disks. Among the higher-point graphs many will contain the graphs in (20), (21), or (22) as disjoint subgraphs, and will therefore give zero integrals. The existence of integrals with zero values can be related directly to the values of Mayer's star integrals. Evidently there are linear relations among some of these integrals; for example,

TABLE I. Values of B_5 and the five-point modified star integrals for hard spheres and hard disks.

Star	Coefficient in B_5	Unlabeling factor[a]	Values of the integrals[b]/b^4 Spheres	Values of the integrals[b]/b^4 Disks	Contribution to B_5/b^4 Spheres	Contribution to B_5/b^4 Disks
∅	6/30	1	$+(7.11\pm0.01)\times10^{-1}$	$+(1.809\pm0.002)$	+0.1422	+0.3618
	−45/30	6	$+(2.092\pm0.009)\times10^{-2}$	$+(1.77\pm0.01)\times10^{-2}$	−0.0314	−0.0266
	60/30	7	$-(8.25\pm0.05)\times10^{-3}$	$-(5.11\pm0.05)\times10^{-3}$	−0.0165	−0.0102
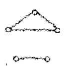	−10/30	1	$+(7.1\pm0.4)\times10^{-4}$	0	−0.0002	0.0000
	−12/30	1	$-(4.05\pm0.03)\times10^{-2}$	$-(2.15\pm0.03)\times10^{-2}$	+0.0162	+0.0086
Values for B_5/b^4:			$+0.1103\pm0.0003$	$+0.3338\pm0.0005$	+0.1103	+0.3336

[a] The unlabeling factor is the number of ways a modified star graph can be labeled and still satisfy the Monte Carlo trial configuration conditions, $f_{12}=f_{23}=f_{34}=f_{45}=-1$.

[b] B_5 and the modified star integrals for spheres (disks) are calculated from 81 (50) independent batches, each of which contains 100 000 Monte Carlo trial configurations. Each modified star integral is the average of a number (unlabeling factor) of topologically identical but differently labeled star integrals. This is equivalent to evaluating a particular labeled star integral using a number of trial configurations equal to (100 000×unlabeling factor) for each batch.

for hard disks, (20) implies the following linear relation:

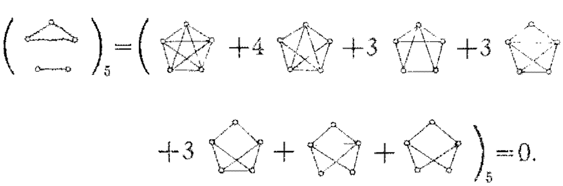

(23)

The linear relations among Mayer's six-point star integrals can be obtained from Table VII, Appendix I. We can use Relation (23) to evaluate the complete star integral if the values of the other integrals in (23) are known. It must be emphasized that (20), (21) and (22) depend on the nature of the interparticle potential ϕ_{ij} (disks); other forms of ϕ_{ij} can lead to other relations.[10] In addition to the integrals in (20), (21), and (22), there are modified integrals which do not appear in the virial expansion that nonetheless vanish and lead to linear relations such as (23). For disks we cite three examples:

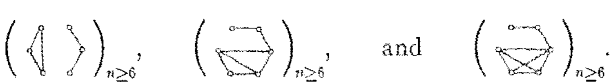

[10] For the hard-square model used by Hoover and De Rocco,[7] the modified star integral,

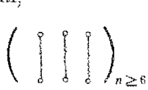

is zero, in addition to the integrals appearing in (20), (21), and (22).

Next, we consider a three-dimensional system of hard spheres with diameter σ. All contributing modified star integrals with four or five points are geometrically allowed. Of the six-point modified diagrams, one diagram contributing to B_6 is zero for geometrical reasons (see Appendix II),

(24)

For graphs with larger $n>6$, more modified stars have zero valued integrals.

4. MONTE CARLO CALCULATIONS

According to Relations (20), (21), and (22), some of the integrals required for evaluating B_5 and B_6 are zero. Therefore, we can limit our attention to the remaining integrals. For spheres, it is necessary to evaluate 5 and 22 modified star integrals for B_5 and B_6, respectively; for disks the corresponding numbers are 4 and 15. These integrals present formidable geometrical problems in 8-, 10-, 12-, and 15-dimensional spaces. We therefore evaluate them by a Monte Carlo method using an IBM 7090 computer. To make a "trial configuration" we place Particle 1 at the origin and Particles 2, ⋯, n randomly within a circle or sphere of diameter $(2n-2)\sigma$, with the conditions $f_{i,i+1}=-1$ for $i=1$, ⋯, $n-1$. Next, the remaining distances between pairs of particles are checked to see if any modified stars occurring in B_5 or B_6 correspond to this

TABLE II. Values of B_6 and the six-point modified star integrals for hard spheres and hard disks.

Star	Coefficient in B_6	Unlabeling factor[a]	Values of the integrals[b]$/b^5$		Contribution to B_6/b^5	
			Spheres	Disks	Spheres	Disks
	−24/144	1	$-(3.53\pm0.01)\times10^{-1}$	$-(1.375\pm0.003)$	+0.0588	+0.2292
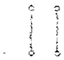	540/144	21	$-(5.66\pm0.04)\times10^{-3}$	$-(7.28\pm0.06)\times10^{-3}$	−0.0212	−0.0273
	−240/144	5	$+(2.0\pm0.1)\times10^{-4}$	$+(2.0\pm0.7)\times10^{-5}$	−0.0003	−0.0000
	−1440/144	54	$+(1.87\pm0.01)\times10^{-3}$	$+(1.91\pm0.02)\times10^{-3}$	−0.0187	−0.0191
	360/144	19	$-(4.2\pm0.1)\times10^{-4}$	$-(3.6\pm0.1)\times10^{-4}$	−0.0011	−0.0009
	900/144	35	$-(3.47\pm0.08)\times10^{-4}$	$-(1.59\pm0.07)\times10^{-4}$	−0.0022	−0.0010
	240/144	10	$-(1.05\pm0.07)\times10^{-4}$	0	−0.0002	0.0000
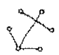	360/144	10	$-(1.07\pm0.02)\times10^{-3}$	$-(7.7\pm0.3)\times10^{-4}$	−0.0027	−0.0019
	360/144	45	$+(3.39\pm0.07)\times10^{-4}$	$+(1.59\pm0.05)\times10^{-4}$	+0.0008	+0.0004
	−180/144	5	$+(5.3\pm0.3)\times10^{-4}$	$+(4.0\pm0.3)\times10^{-4}$	−0.0007	−0.0005
	288/144	8	$+(4.93\pm0.05)\times10^{-3}$	$+(4.51\pm0.07)\times10^{-3}$	+0.0099	+0.0090
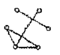	−540/144	16	$+(6.6\pm0.5)\times10^{-5}$	0	−0.0002	0.0000
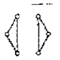	−40/144	1	0	0	0.0000	0.0000
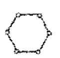	−240/144	5	$-(1.03\pm0.08)\times10^{-4}$	-10^{-6}	+0.0002	+0.0000
	−360/144	24	$-(6.2\pm0.4)\times10^{-5}$	0	+0.0002	0.0000
	−1080/144	24	$-(1.76\pm0.02)\times10^{-3}$	$-(1.17\pm0.02)\times10^{-3}$	+0.0132	+0.0088
	180/144	3	$-(2.0\pm0.6)\times10^{-5}$	0	−0.0000	0.0000
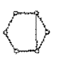	720/144	12	$+(2.46\pm0.10)\times10^{-4}$	$+(1.3\pm0.3)\times10^{-5}$	+0.0012	+0.0001
	90/144	4	$+(1.3\pm0.5)\times10^{-5}$	0	+0.0000	0.0000
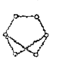	360/144	8	$+(4.83\pm0.06)\times10^{-3}$	$+(3.09\pm0.07)\times10^{-3}$	+0.0121	+0.0077
	−15/144	0	negligible	0	−0.0000	0.0000
	−180/144	2	$-(2.8\pm0.3)\times10^{-4}$	0	+0.0004	0.0000
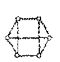	−60/144	1	$+(2.62\pm0.04)\times10^{-2}$	$+(1.23\pm0.04)\times10^{-2}$	−0.0109	−0.0051
Values for B_6/b^5:			$+0.0386\pm0.0004$	$+0.1992\pm0.0008$	+0.0386	+0.1994

[a] The unlabeling factor is the number of ways a modified star graph can be labeled and still satisfy the Monte Carlo trial configuration conditions, $f_{12}=f_{23}=f_{34}=f_{45}=f_{56}=-1$.

[b] B_6 and the modified star integrals for spheres (disks) are calculated from 60 (38) independent batches, each of which contains 100 000 Monte Carlo trial configurations. Each modified star integral is the average of a number (unlabeling factor) of topologically identical but differently labeled star integrals. This is equivalent to evaluating a particular labeled star integral using a number of trial configurations equal to (100 000×unlabeling factor) for each batch.

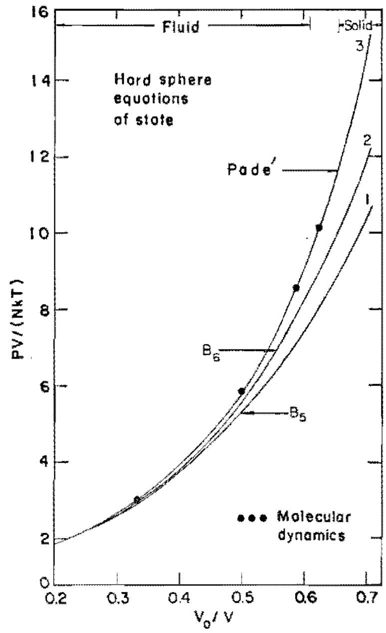

FIG. 2. Plot of $PV/(NkT)$ versus V_0/V for hard spheres. V_0 is the volume at closest-packing $N\sigma^3/\sqrt{2}$. The curves are: (1) virial series including B_5, (2) virial series including B_6, and (3) a Padé approximant. Molecular dynamics results of Alder and Wainwright (Ref. 12) are indicated by ●●●.

particlar trial configuration. For example,

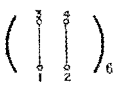

can be evaluated according to the following recipe:

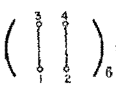
$= (2b)^5(-)^{13}$

$\times$(number of occurrences of 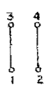 / number of trials).

(25)

In (25), b is B_2, $(2\pi/3)\sigma^3$ for spheres and $(\pi/2)\sigma^2$ for disks; the factor $(-)^{13}$ corresponds to the number of f functions in (25). In practice the (20) other possible labelings of 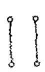 consistent with $f_{12}=f_{23}=f_{34}=f_{45}=f_{56}=-1$ are counted too, and the corresponding integrals are averaged. We call the number of ways a wiggly-line graph can be labeled subject to the restriction $f_{12}=f_{23}=f_{34}=f_{45}=f_{50}=-1$ the "unlabeling factor" for that graph. The corresponding unlabeling factors for the other modified star graphs are listed in Tables I and II. The unlabeling improves the efficiency of the Monte Carlo method. Of the modified stars contributing to B_6, only the configuration 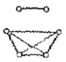 cannot be constructed with the type of trial configuration we have just described. We attempted to evaluate this integral separately. Trial configurations were selected with the following restriction:

$$f_{13}=f_{14}=f_{15}=f_{16}=f_{23}=f_{24}=f_{25}=f_{26}=-1;$$

$$1\leq r_{12}<\sqrt{2}(\sigma\equiv 1). \quad (26)$$

Out of 210 000 such configurations none satisfied the required configuration. From this we conclude that this modified star integral is orders of magnitude smaller than those which we evaluated. We omit this type of wiggly-line integral from the B_6 calculation with an error negligible relative to the uncertainty in our final result.

Tables I and II give the results and expected errors of the Monte Carlo calculations. The error for any Monte Carlo integral I is estimated by the following formula[11]:

$$\text{error}=\left[\sum_{i=1}^{q}(\langle I_i\rangle-\langle I\rangle)^2/(q(q-1))\right]^{\frac{1}{2}}, \quad (27)$$

where $\langle I\rangle$ is the final Monte Carlo average of I as obtained from q independent Monte Carlo averages $\langle I_i\rangle$ $(i=1, \cdots, q)$ over batches of trial configurations. The number of independent batches, q, and the number of random Monte Carlo trial configurations in each batch are given in Tables I and II. The estimated errors are essentially independent of q for the same total number of Monte Carlo trial configurations. Each of these Monte Carlo trial configurations satisfies the restrictions of at most one of the modified stars contributing to the virial coefficient expressions (10) and (11).

5. DISCUSSION

Several aspects of the modified star integrals given in Tables I and II are notable. First, the complete star integrals have the largest absolute values of all the star integrals shown. The complete star integrals always make positive contributions to the virial coefficients. Second, the next seven modified star integrals contributing to B_6 (Table II) give nonpositive corrections. The net negative correction made by these terms

[11] The mean-square expected deviation of a quantity from the exact value I is $\langle(\langle I\rangle-I)^2\rangle$, where $\langle\ \ \rangle$ denotes the expectation operator, and $\langle I\rangle$ is the final average value over q independent values, $\langle I_i\rangle$, in the present problem. However, this deviation is equal to σ^2/q, where σ is the variance of I. For a finite number of batches, σ can be approximated by $\bar{\sigma}$ defined in a finite number of batches, i.e., $\bar{\sigma}^2=[(q-1)/q]\sigma^2$ [see P. G. Hoel, *Introduction to Mathematical Statistics* (John Wiley & Sons, Inc., New York, 1954), 2nd ed., p. 198].

contributes significantly to B_6, and may become large enough to give negative B_n for larger values of n, because the factors multiplying these graphs increase rapidly with n. Third, the next largest integrals among the modified star integrals are the ring graphs, which are formed by n f functions and $\frac{1}{2}n(n-3)\tilde{f}$ functions. These integrals give positive (negative) contributions to B_n if n is odd (even). Fourth, we see that the three-dimensional modified star integrals which are zero in two dimensions have much smaller values than the other three-dimensional modified star integrals. If only the complete star graphs are used to calculate B_5 and B_6 for disks ("one-dimensional approximation"), the values of B_5/b^4 and B_6/b^5 are, respectively, 8.4% and 15% larger than the values given in Tables I and II. If we include for spheres only those integrals which are not zero for disks ("two-dimensional approximation") B_5/b^4 and B_6/b^5 are, respectively, 0.21% larger and 0.17% smaller than our calculated values.

If the virial series converges to the true pressure in the density range of the first-order fluid-solid phase transition,[12,13] some of the higher virial coefficients must necessarily be negative in order to describe a flat or looped isotherm in the P–V diagram. It is interesting therefore to know the density range within which the five- or six-term virial series is a good approximation to the complete infinite series. In Figs. 2 and 3,

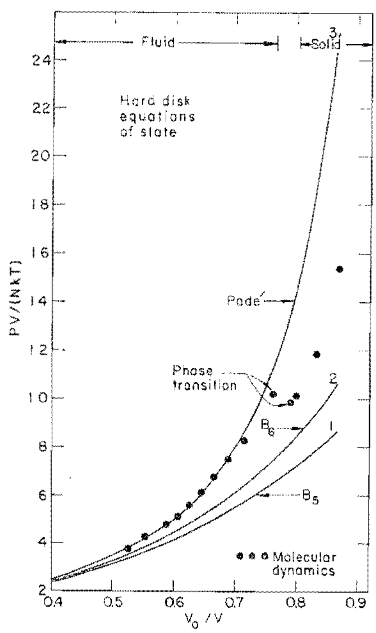

FIG. 3. Plot of $PV/(NkT)$ versus V_0/V for hard disks. V_0 is the volume at closest-packing, $N\sigma^2\sqrt{3}/2$. The curves are: (1) virial series including B_5, (2) virial series including B_6, and (3) a Padé approximant. Molecular dynamics results of Alder and Wainwright (Ref. 13) are indicated by ●●●.

[12] B. J. Alder and T. E. Wainwright, J. Chem. Phys. **33**, 1439 (1960).

[13] B. J. Alder and T. E. Wainwright, Phys. Rev. **127**, 359 (1962). The additional data given in Fig. 3 and Table IV are kindly supplied to us by these authors.

TABLE III. Values of $PV(NkT)$ obtained by using the five- and the six-term virial series, a Padé approximant, and the molecular dynamics results (MD) on the fluid branch of the equation of state for hard spheres ($V_0=N\sigma^3/\sqrt{2}$).

V/V_0	Five-term series	Six-term series	Padé	MD[a]
1.60	8.11	8.95	10.11	10.17[b]
1.70	7.17	7.79	8.55	8.59
2.00	5.31	5.59	5.83	5.89
3.00	2.98	3.01	3.03	3.05
10.00	1.36	1.36	1.36	1.36

[a] These data for systems of 108 spheres were kindly furnished by B. J. Alder and T. E. Wainwright.

[b] At this density, both solid and fluid phases can occur for a system with a finite number of particles. The phase transition from the fluid to the solid for a system with an infinite number of particles is estimated to start at $V/V_0\approx 1.63$.

these series are plotted together with the molecular dynamics data of Alder and Wainwright.[12,13] Figures 2 and 3 also show the plots obtained by Padé approximants (see Appendix III), $P(3,3)$, to $PV^2/(N^2kT)-V/N$, using the known values of B_2 through B_6:

$$\text{spheres: } \frac{V}{N}\left[\frac{PV}{NkT}-1\right]\doteq P(3,3)$$

$$\equiv\frac{b(1+0.063507b\rho+0.017329b^2\rho^2)}{(1-0.561493b\rho+0.081313b^2\rho^2)}; \quad (28)$$

$$\text{disks: } \frac{V}{N}\left[\frac{PV}{NkT}-1\right]\doteq P(3,3)$$

$$\equiv\frac{b(1-0.196703b\rho+0.006519b^2\rho^2)}{(1-0.978703b\rho+0.239465b^2\rho^2)}. \quad (29)$$

In the case of disks, the six-term virial series pressure is considerably below (25%) the molecular dynamics pressure on the fluid side of the two-phase region ($V=1.312V_0$). We therefore expect the next several coefficients for disks to be positive. It is interesting, but probably not significant, to note that the sphere B_n from (28) are given by

$$\text{spheres: } B_{n+3\geq 3}/b^{n+2}=0.28515^n[0.62500\cos(0.17606n)$$
$$+2.2603\sin(0.17606n)]. \quad (30)$$

From (30) we see that B_{20} has the first negative sign, and the sign of the sphere B_n changes roughly every 16 terms, while the disk B_n from (29) are all positive,

$$\text{disks: } B_{n+3\geq 3}/b^{n+2}=0.48935^n[0.78200+0.30597^n]. \quad (31)$$

Strangely enough, the denominator of (29) is (to six significant figures), a perfect square $(1-0.489351b\rho)^2$. We note that values of the six-term virial series agree within 1% with the molecular dynamics results for hard spheres and disks at volumes greater than twice

TABLE IV. Values of $PV/(NkT)$ obtained by using the five- and six-term virial series, a Padé approximant, and the molecular dynamics results (MD) on the fluid branch (Ref. 13) of hard disks. ($V_0=N\sigma^2\sqrt{3}/2$).

V/V_0	Five-term series	Six-term series	Padé	MD
1.312[a]	6.50	7.51	11.11	10.13
1.40	5.71	6.44	8.45	8.25
1.45	5.33	5.95	7.45	7.47
1.50	5.01	5.52	6.66	6.67
1.55	4.72	5.16	6.03	6.08
1.60	4.47	4.84	5.52	5.56
1.65	4.24	4.56	5.10	5.13
1.70	4.04	4.31	4.74	4.76
1.80	3.69	3.90	4.18	4.24
1.90	3.41	3.57	3.76	3.78
2.00	3.17	3.30	3.43	3.39

[a] The phase transition from the fluid to the solid for a system with an infinite number of particles is estimated to start at $V/V_0=1.312$.

closest-packed. The values of the Padé approximants agree even better with the dynamics data. The agreement with the fluid branch is good even at phase-transition densities (Tables III and IV). However, the Padé approximants do not show any maxima or minima on the P–V diagram.

The Padé approximant method has proved to be very accurate in estimating critical parameters for Ising lattice problems.[14–17] If the Padé approximants (28) and (29) are used to estimate B_7 and B_8, the following values are obtained[18]:

spheres: $B_7/b^6=0.0127$, and $B_8/b^7=0.0040$, (32)

disks: $B_7/b^6=0.115$, and $B_8/b^7=0.065$. (33)

By subtracting the six-term virial series from the molecular dynamics $PV/(NkT)$ (Tables III and IV) and assuming the remainder can be represented by the single term $B_7\rho^6$, we find:

$$\text{Spheres: } B_7/b^6\approx 0.03, \quad (34)$$

$$\text{Disks: } B_7/b^6\approx 0.3. \quad (35)$$

The exact evaluation of B_7 by integrating the modified star integrals occurring in V_7 is now in progress for both spheres and disks.

[14] G. A. Baker, Jr., Phys. Rev. **124**, 768 (1961).
[15] J. W. Essam and M. E. Fisher, J. Chem. Phys. **38**, 802 (1963).
[16] P. Heller and G. B. Benedek, Phys. Rev. Letters **8**, 428 (1962).
[17] C. Domb and M. F. Sykes, J. Math. Phys. **2**, 63 (1961); **3**, 586 (1962).
[18] The Padé approximant, $P(1, 2)$, gives $B_6/b^5=0.0364$ for spheres and $B_6/b^5=0.1974$ for disks. These values agree well with the exact values obtained in this paper: 0.0386 and 0.1992, respectively.

6. ACKNOWLEDGMENTS

We wish to thank Dr. Donald H. Davis for illuminating discussions on the Monte Carlo calculations and Mr. Warren G. Cunningham for programming the Monte Carlo problem for the IBM 7090. We would like to acknowledge interesting discussions with Dr. S. Katsura, Dr. J. E. Kilpatrick, and Dr. J. S. Rowlinson on the general problem of hard-sphere virial coefficient calculations. Katsura's calculation of the hard-sphere B_5 has been published in *The Journal of Chemical Physics.*

APPENDIX I

This appendix gives the detailed transformation of the star integrals into modified star integrals. To the right of each labeled star type are listed the modified stars arising from it. The number of ways each type of star can be labeled is taken into account so that the entries in Tables V–VII give the total number of times each modified star integral appears when *all* of the Mayer labeled stars are expanded and the contributions added together.

TABLE V. Transformation of the four-point labeled stars to modified stars.

Labelings	Star	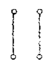		∅
3	□	3	−6	3
6	▨		6	−6
1	⊠			1
Totals		3	0	−2

APPENDIX II

In this appendix we prove that three distinct modified star integrals are zero.

Proof 1:

$$\left(\quad \right)_{n\geq 5}=0.$$
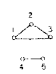

For convenience we take the disk diameter to be unity. In Fig. 4 circles with unit radius, centered on Particles 1 and 2 are drawn. Particle 3 must lie outside these circles in order to satisfy $\tilde{f}_{13}\tilde{f}_{23}\neq 0$. Particles 4 and 5 ($\tilde{f}_{45}\neq 0\rightarrow r_{45}>1$) must satisfy the conditions

$$r_{14},\quad r_{15},\quad r_{24},\quad \text{and}\quad r_{25}\leq 1, \quad (36)$$

$$r_{34}\quad \text{and}\quad r_{35}\leq 1. \quad (37)$$

TABLE VI. Transformation of the five-point labeled stars to modified stars.

Labelings	Star			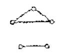					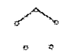	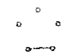	∅
12		12	−60			60	60	−60	−60	60	−12
60			60			−120	−120	180	180	−240	60
10				10	−10		−30	30	30	−40	10
10					10				−30	30	−10
60						60		−60	−120	180	−60
30	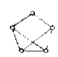						30	−60	−30	90	−30
15	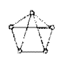							15		−30	15
30									30	−60	30
10	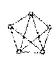									10	−10
1											1
Totals		12	0	10	0	0	−60	45	0	0	−6

Equation (36) restricts 4 and 5 to be within the area common to the two unit circles, and the condition $r_{45}>1$ implies $r_{12}<\sqrt{3}$. The optimum position for Particle 3 which will still satisfy (37) is denoted by A (or A′) in Fig. 4. Particles 4 and 5 must then be located in the shaded area ABCA to satisfy (36) and (37). However, this optimum configuration cannot satisfy $r_{45}>1$. Consequently, the corresponding integral is zero. This proof is equally valid for any $n\geq 5$. Direct applications of the proof lead easily to other identities such as (21) involving the present integral.

Proof 2:

(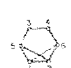)$_{n\geq 6}=0.$

Referring to Fig. 4, we have the condition $1\leq r_{12}<\sqrt{3}$ because $r_{34}(>1)$ must lie within the area A′BACA′ common to the two unit circles. The restrictions r_{15}, r_{16}, r_{25}, and $r_{26}\geq 1$ place Particles 5 and 6 outside both unit circles in Fig. 4. Evidently 5 and 6 must both lie below or above the unit circles to satisfy $r_{56}<1$. We place them below, in the vicinity of A. But, since both r_{36} and r_{45} must be less than unity, Particles 3 and 4 must lie inside the shaded area ABCA. This violates the condition $r_{34}>1$. Therefore, the integral corresponding to the above configuration is zero. The proof is equally valid for any $n>6$.

Proof 3:

(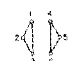)$_{n\geq 6}=0.$

It can be shown that the area of any cross section within the volume common to three unit spheres centered at the points 1, 2, and 3 (and satisfying r_{12}, r_{13}, and $r_{23}>1$) is contained in an area common to two unit circles whose centers are separated by at least unit distance. However, we cannot place the triangle 456 (with r_{45}, r_{46}, and $r_{56}>1$) inside such an area. Therefore, the corresponding integral is zero. This proof is equally valid for any $n>6$.

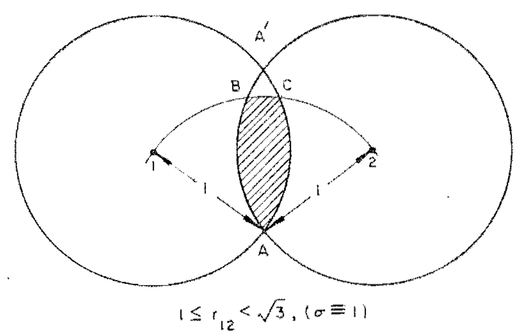

FIG. 4. Disk geometry. Unit circles are centered on Particles 1 and 2 with $1\leq r_{12}<\sqrt{3}$.

TABLE VII. Transformation of the six-point labeled stars to

Labeling																													
60	1	60	-360	-180				720	360	180		360	180	360			-120	-360	-360	-360	-360	-720		-720	-1080	-720	-180	-60	
360	2		360					-720	-720	-360		-720		-360			360	720	720	720	360	1440		2160	2520	720	360		
180	3			180				-720					-360	-360				360	360	360	720	720			720	1440	180	180	
180	4				180	-180					-360	-180		-720		360				180		1440	180	360	1080	1080	360		-180
180	5					180										-360				-180		-720							180
15	6						15								-15								-90						90
720	7							720										-720	-720	-720	-720	-720			-720	-720			
360	8								360								-360		-360			-720		-720	-360				
180	9									180								-360						-720			-180		
360	10										360					-360						-720	-360	-360		-720			360
180	11											180								-180				-360	-720				
90	12												90								-180					-360		-90	
360	13													360								-720			-720	-720	-360		
15	14														15														-90
360	15															360													-360
120	16																120												
360	17																	360											
360	18																		360										
180	19																			180									
180	20																				180								
720	21																					720							
90	22																						90						-90
360	23																							360					
360	24																								360				
360	25																									360			
60	26																										60		
10	27																											10	
90	28																												
360	29																												
90	30																												
360	31																												
360	32																												
360	33																												
360	34																												
180	35																												
72	36																												
45	37																												
360	38																												
60	39																												
180	40																												
360	41																												
45	42																												
60	43																												
360	44																												
60	45																												
180	46																												
90	47																												
60	48																												
20	49																												
180	50																												
180	51																												
15	52																												
60	53																												
45	54																												
15	55																												
1	56																												
Totals		60	0	0	180	0	15	0	0	0	0	-360	-90	-720	0	0	0	0	0	0	0	0	-180	0	1080	360	240	40	0

[a] The above 56 types of six-point stars are listed in the same order as in Appendix I of Ref. 7.

modified stars. The lines in the graphs represent wiggly lines.[a]

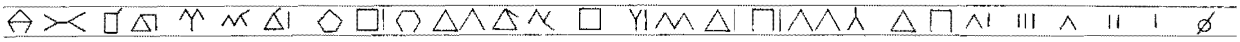

360	180	720	720	1080	1440	360	360	150	1800	360	-360	-1440	-180	-360	-2520	-360	-1140	-900	360	120	1800	2520	240	-1080	-1080	540	-60
-1080	-360	-2160	-1440	-3600	-3600	-720	-1080	-720	-5040	-360	1080	5040	720	1080	8640	720	5400	2520	-1440	-360	-7560	-9720	-1080	5040	5040	-2880	360
-360	-360	-720	-1440	-720	-2160	-720	-360		-2160	-1080	720	2160	180	720	3960	1080	1800	1980	-720	-360	-3240	-5400	-360	2520	2520	-1440	180
-720		-360	-1080	-1080	-1800	-1080	-360	-150	-2880	-360	1080	1800	180	720	3960	720	2700	1440	-720	-360	-3420	-5040	-540	2520	2520	-1440	180
720		360	720	360	720	360			360		-1080	-1440	-180	-360	-1800	-360	-720	-360	720	360	2520	2520	180	-2160	-1620	1260	-180
						180		45			-180		-45	-60		-60	-180		60	60	180	180	45	-180	-135	105	-15
720	720	2160	2160	1440	3600	720	720		2160	720	-1440	-5760	-720	-1440	-8640	-1440	-2880	-2880	2160	720	9360	12240	720	-7920	-7200	5040	-720
1080		720	720	1800	720	360	360	360	1440		-1080	-2880	-360	-360	-3960	-360	-2880	-720	1080	360	5040	5400	720	-3960	-3600	2520	-360
	180	720		1080				360	1440			-1440	-360		-1800		-2160	-540	360		2520	2880	540	-1800	-1980	1260	-180
720		360	1080	720	720	1440		360	1440	360	-1800	-1800	-360	-720	-2880	-1080	-2880	-1080	1080	720	4320	5760	720	-3960	-3600	2520	-360
		360		720	1080		360	180	1080			-1080	-180	-360	-2520		-1440	-720	360		2340	3240	360	-1800	-1980	1260	-180
	90		360		360	180			360	540	-180	-360		-180	-720	-540	-360	-810	180	180	720	1980	90	-900	-990	630	-90
360			720	720	1440	720	360		2880	360	-720	-1440		-720	-4320	-720	-2880	-1800	720	360	3960	6840	720	-3600	-3960	2520	-360
											180		45						-60	-60	-180			180	45	-90	15
-720		-360	-720								1800	1440	360		1440	360			-1080	-720	-3600	-1800		3600	1800	-2160	360
-360				-360							360	720			360		360		-360	-120	-1080	-720	-120	1080	720	-720	120
	-360	-720		-720					-360			2160	360		1440		1080	360	-720		-3240	-2880	-360	2880	2520	-2160	360
-360		-720	-720				-360				720	1440	360		2520	360			-720	-360	-3600	-2520		3240	2160	-2160	360
		-360			-720							720	180	360	1080			360	-360		-1440	-1800		1440	1260	-1080	180
	-180		-360		-360					-180	180	720		180	720	360		540	-360	-180	-1080	-1980		1440	1260	-1080	180
-720			-720	-720	-720	-720			-720		1440	2160		720	2880	720	2160	720	-1440	-720	-5040	-6480	-720	5760	5040	-4320	720
						-360		-90			360		90	180		180	540		-160	-180	-540	-720	-180	720	630	-540	90
		-360		-720				-360	-720			1080	360		1440		2160	360	-360		-2880	-3240	-720	2520	2880	-2160	360
				-360	-720		-360		-720			720		360	2520		1080	720	-360		-2520	-3960	-360	2520	2880	-2160	360
			-360		-360	-360			-720	-360	360	360		360	1440	720	1080	1080	-360	-360	-1800	-4320	-360	2520	2880	-2160	360
									-360						360		360	180			-360	-720	-120	360	540	-360	60
										-60						60		90		-20		-180		60	90	-60	10
											-360		-90						180	180	540			-720	-180	450	-90
360											-720	-720			-360				720	360	1800	720		-2520	-1080	1800	-360
	90											-360						-90	180		360	360		-540	-360	450	-90
		360										-720	-360		-720				360		2160	1080		-2160	-1440	1800	-360
			360								-360	-360			-720	-360			360	360	1440	1440		-2160	-1440	1800	-360
				360								-720			-360		-720		360		1440	1440	360	-1800	-1800	1800	-360
					360							-360		-360	-720			-360	360		1080	2160		-1800	-1800	1800	-360
						180					-180			-180		-180	-360		180	180	360	900	180	-900	-900	900	-180
							72								-360						360	360		-360	-360	360	-72
								45					-45				-180				180	180	90	-180	-270	225	-15
									360						-720		-720	-360			1080	2160	360	-1440	-2160	1800	-360
										60						-120		-160		60		540		-240	-360	300	-60
											180								-180	-180	-360			900	180	-720	180
												360							-360		-720	-360		1440	720	-1440	360
													45								-180			180	90	-180	45
														60					-60			-180		180	180	-240	60
															360						-720	-720		1080	1080	-1440	360
																60				-60		-180		180	180	-240	60
																	180				-180	-360	-180	360	720	-720	180
																		90				-360		180	360	-360	90
																			60					-180		180	-60
																				20				-60		60	-20
																					180			-360	-180	540	-180
																						180		-180	-360	540	-180
																							15		-45	45	-15
																								60		-120	60
																									45	-90	45
																										15	-15
																											1
0	0	0	0	0	0	540	-288	180	-360	0	0	0	0	-360	0	-240	-900	-360	0	0	0	1440	240	0	-540	0	24

APPENDIX III

This appendix indicates the general method for obtaining Padé approximants to the virial series.

We define the Padé approximant to $PV^2/(N^2kT)-V/N$ by the relation

$$P(n,m)=\sum_{i=1}^{n}a_i\rho^{i-1}\Big/\sum_{i=1}^{m}\alpha_i\rho^{i-1},\quad a_1\equiv B_2,\quad \alpha_1\equiv 1,\tag{38}$$

where n and m are positive integers and the expansion of (38) reproduces the virial coefficients up to B_{n+m}. The virial expansion of $PV^2/(N^2kT)-V/N$ is given by the following equation,

$$[PV/(NkT)-1](V/N)=\sum_{i=1}^{\infty}B_{i+1}\rho^{i-1}.\tag{39}$$

The coefficients a_i and α_i can be evaluated from (38) and (39), which can be written in the equivalent form:

$$\begin{array}{c}\overset{\longleftarrow\; n-1\;\longrightarrow\qquad\longleftarrow\; m-1\;\longrightarrow}{}\\ \begin{array}{c} n-1\\ \\ m-1\end{array}\begin{pmatrix}1 & 0 & \cdots & 0 & -B_2 & 0 & \cdots & 0\\ 0 & 1 & \cdots & 0 & -B_3 & -B_2 & \cdots & 0\\ \cdots & \cdots & \cdots & \cdots & \cdots & \cdots & \cdots & \cdots\\ 0 & \cdots & \cdots & 1 & -B_n & -B_{n-1} & \cdots & \cdots\\ 0 & \cdots & \cdots & 0 & -B_{n+1} & -B_n & \cdots & \cdots\\ 0 & \cdots & \cdots & \cdots & \cdots & \cdots & \cdots & \cdots\\ 0 & \cdots & \cdots & 0 & -B_{n+m-1} & -B_{n+m-2} & \cdots & -B_n\end{pmatrix}\end{array}\begin{pmatrix}a_2\\ a_3\\ \vdots\\ a_n\\ \alpha_2\\ \vdots\\ \alpha_m\end{pmatrix}=\begin{pmatrix}B_3\\ B_4\\ \vdots\\ B_{n+1}\\ B_{n+2}\\ \vdots\\ B_{n+m}\end{pmatrix}\tag{40}$$

The recursion relation

$$B_k=-\sum_{i=2}^{m}B_{k+1-i}\alpha_i,\qquad k\geq n+2\tag{41}$$

can be used to estimate higher virial coefficients.